

# Influence of Chain Microstructure on the Crystallization Kinetics of Metallocene-Made Isotactic Polypropylene

Claudio De Rosa,<sup>\*,†</sup> Finizia Auriemma,<sup>†</sup> and Luigi Resconi<sup>‡</sup>

Dipartimento di Chimica, Università di Napoli "Federico II", Complesso Monte S. Angelo, Via Cintia, 80126 Napoli, Italy, and Basell Polyolefins, Centro Ricerche G. Natta, P.le G. Donegani 12, I-44100 Ferrara, Italy

Received May 27, 2005; Revised Manuscript Received September 19, 2005

**ABSTRACT:** Highly regioregular isotactic polypropylene samples containing only *rr* defects of stereoregularity in a wide range of concentration have been obtained with a series of regiospecific metallocene catalysts. A study of the relationships between kinetics of melt-crystallization and the microstructure of polypropylene chains is reported. The equilibrium melting temperatures for isotactic polypropylenes of different stereoregularity have been estimated. The kinetic study has shown that the crystallization rate increases with increasing the concentration of *rr* defects and decreasing the molecular weight. During isothermal crystallizations from the melt, crystals of  $\alpha$  form develop at the beginning of the crystallization, whereas the formation of crystals of  $\gamma$  form is observed only at longer crystallization times. According to the literature, the crystals of  $\gamma$  form are nucleated over the preformed crystals of  $\alpha$  form.

## Introduction

With the development of metallocene catalytic systems for the isospecific polymerization of olefins, new isotactic polypropylenes, showing a wide variety of microstructures, have become available.<sup>1</sup> Depending on the specific metallocene catalyst, as well as on the polymerization conditions (i.e., monomer concentration, temperature, nature of cocatalyst, etc.), isotactic polypropylene (i-PP) samples containing different amounts and combinations of defects of stereoregularity (primary insertions with the wrong enantioface, or stereodefects) and regioregularity (*meso* and *racemo* secondary insertions, or regiodefects) can be obtained.<sup>1</sup> It has been shown that the microstructure strongly influences the crystallization properties of i-PP and its polymorphic behavior.<sup>2–17</sup> In particular, the crystallization of  $\alpha$  and  $\gamma$  forms depends on the stereoregularity and, in general, on the concentration of stereo- and regiodefects<sup>2–4,7,9–12,15–17</sup> and on the distribution of defects along the polymer chains.<sup>10,12–14</sup>

We have recently studied the crystallization behavior and the physical properties of metallocene-made i-PP samples containing only one kind of stereo-irregularity (isolated *rr* triads), in a wide range of concentration.<sup>16,17</sup> This study has allowed clarifying the single effect of the presence of *rr* defects on the polymorphic behavior and mechanical properties of i-PP.<sup>16,17</sup> This stereodeflect induces crystallization of  $\gamma$  form and of disordered modifications intermediate between  $\alpha$  and  $\gamma$  forms. A linear relationship between the amount of  $\gamma$  form that crystallizes from the melt and the average length of isotactic sequences has been found.<sup>16</sup> Depending on the concentration of *rr* defects, polypropylenes with melting temperatures variable from 160 to 80 °C and mechanical properties intermediate between those of stiff-plastic and elastomeric materials have been produced.<sup>16,17</sup>

All these studies have indicated that the crystallization of  $\gamma$  form seems to be thermodynamically favored in samples containing an appreciable amount of stereo-defects. As a consequence, a high amount of  $\gamma$  form develops in the slow crystallizations at high temperatures. However, it has also been demonstrated that even for samples with high concentration of defects, high concentration of the  $\alpha$  form may be obtained when the crystallization is very fast, for instance by quenching the melt to room temperature,<sup>11</sup> indicating that for these samples the  $\alpha$  form is kinetically favored. Therefore, the crystallization of  $\alpha$  and  $\gamma$  forms of i-PP in metallocene-made samples containing a random distribution of defects is a result of two competing kinetic and thermodynamic effects.<sup>3,4,11</sup>

In this paper the kinetics of crystallization from the melt of i-PP samples containing only *rr* stereodeflects and free from regiodeflects are analyzed. The effect of the presence of *rr* defects on the overall crystallization rate is studied, independent of the number and the amount of crystalline forms that develop during isothermal crystallizations.

## Experimental Section

i-PP samples have been prepared with the highly regiospecific  $C_2$ - and  $C_1$ -symmetric zirconocene catalysts shown in Chart 1,<sup>18–22</sup> activated with methylalumoxane (MAO). The  $C_2$ -symmetric complexes **1**, *rac*-H<sub>2</sub>C(3-*tert*-butylindenyl)<sub>2</sub>ZrCl<sub>2</sub>, and **2**, *rac*-isopropylidene[bis(3-trimethylsilylindenyl)]ZrCl<sub>2</sub>, have been prepared as described in refs 19 and 18, respectively. The  $C_1$ -symmetric *ansa*-zirconocenes **3–5** are based on the substituted indenyl-dimethylsilyl[bis(2-methylthienocyclopentadienyl)] ligand framework and have been prepared as described in refs 20–22.

All the analyzed i-PP samples are listed in Table 1. The samples show similar molecular weight and different concentrations of *rr* defects. The more isotactic samples iPP1–iPP3 have been prepared with the  $C_2$ -symmetric catalyst **1**,<sup>18,19</sup> whereas samples iPP4–iPP7 have been prepared with the  $C_1$ -symmetric *ansa*-zirconocenes **3–5**,<sup>20–22</sup> which are highly active in propylene polymerization and produce highly regioregular, high molecular weight i-PPs characterized by different stereoregularity, depending on the indenyl substituents.<sup>16,17,22</sup> Sample R3 has been prepared with catalyst **2**/MAO at 60 °C

<sup>†</sup> Università di Napoli "Federico II".

<sup>‡</sup> Basell Polyolefins.

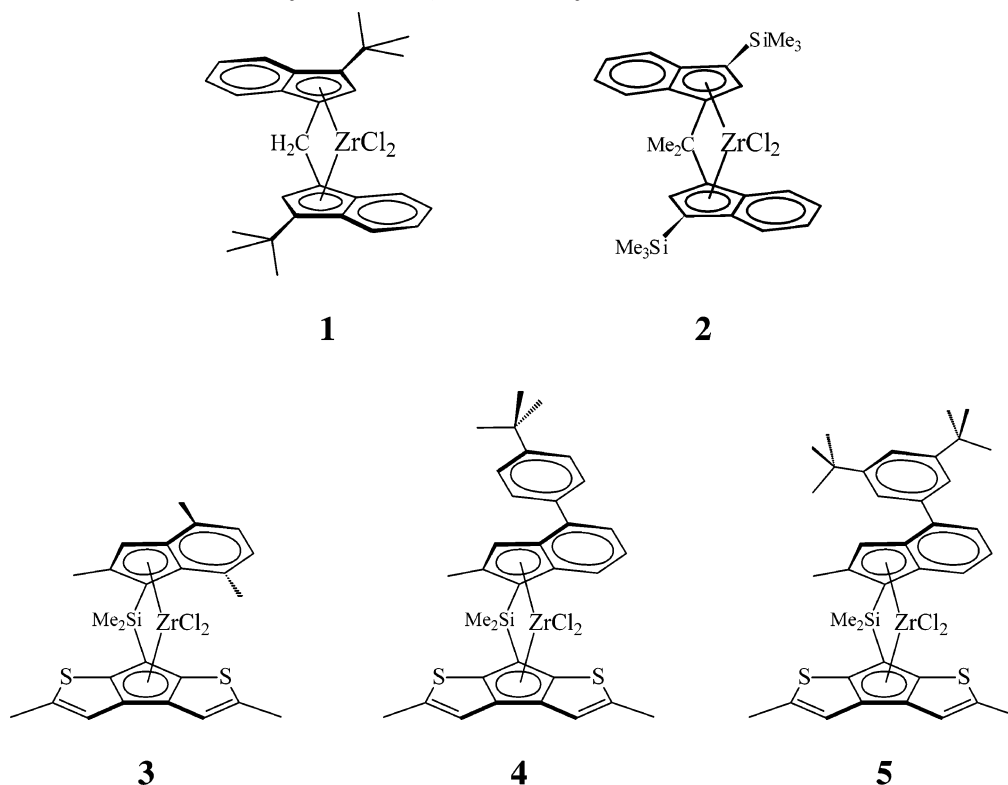
\* To whom correspondence should be addressed: Tel ++39 081 674346; Fax ++39 081 674090; e-mail claudio.derosa@unina.it, derosa@chemistry.unina.it.

**Table 1. Polymerization Temperatures ( $T_p$ ), Melting Temperatures ( $T_m$ ), Average Viscosity Molecular Weights ( $M_v$ ), Content of Triads Stereosequences and of Isotactic *mmmm* Pentad (%), and Equilibrium Melting Temperatures ( $T_m^0$ ) of i-PP Samples Prepared with the Catalysts of Chart 1<sup>a</sup>**

sample	catalyst/cocatalyst/carrier <sup>b</sup>	$T_p$ (°C)	$T_m$ (°C) <sup>c</sup>	$M_v$	<i>mm</i> (%) <sup>d</sup>	<i>mr</i> (%) <sup>d</sup>	<i>rr</i> (%) <sup>d</sup>	<i>mmmm</i> (%) <sup>d</sup>	$T_m^0$ (°C) <sup>e</sup>
iPP1	1/MAO	50	162	195 700	98.52	0.99	0.49	97.55	174.6
iPP2	1/MAO	60	157	108 900	98.05	1.30	0.65	96.77	171.6
iPP3	1/MAO/PE	60	156	120 400	97.46	1.69	0.85	95.81	167.7
iPP4	5/MAO	70	145	161 600	95.92	2.72	1.36	93.29	156.8
iPP5	4/MAO/PE	60	140	106 000	92.37	5.08	2.54	87.61	152.4
iPP6	3/MAO	60	137	222 800	90.45	6.37	3.18	84.59	152.4
R3	2/MAO	60	137	66 000	89.67 <sup>f</sup>	6.89 <sup>f</sup>	3.44 <sup>f</sup>	83.37 <sup>f</sup>	148.0
iPP7	3/MAO/PP	60	133	202 400	88.90	7.40	3.70	82.19	148.0

<sup>a</sup> No or negligible regioerrors (2,1 insertions) could be observed in the <sup>13</sup>C NMR spectra of the samples.<sup>18,22</sup> <sup>b</sup> PE = polyethylene, PP = polypropylene. <sup>c</sup> The melting temperatures were obtained with a differential scanning calorimeter Perkin-Elmer DSC-7 performing scans in a flowing N<sub>2</sub> atmosphere and heating rate of 10 °C/min. <sup>d</sup> Data taken from Table 2 of ref 16. The data have been calculated from the <sup>13</sup>C NMR analysis using the enantiomorphic site model. <sup>e</sup> Equilibrium melting temperatures were obtained by the Hoffman–Weeks<sup>28</sup> extrapolation procedure (see text and Figure 5A). <sup>f</sup> Data taken from ref 18.

**Chart 1. Structures of C<sub>2</sub>-Symmetric (1, 2) and C<sub>1</sub>-Symmetric (3–5) Zirconocene Precatalysts**



in liquid propylene<sup>18</sup> and has a molecular weight lower than those of samples iPP<sub>n</sub> prepared with the catalysts **1** and **3–5**.

All propylene polymerizations have been performed in liquid propylene at polymerization temperatures between 50 and 70 °C, as described in refs 18–22. Some of the MAO-activated complexes were also supported on porous polyethylene and polypropylene spheres by following a Basell technology<sup>23</sup> and tested under the same conditions as the nonsupported system.

Polymer <sup>13</sup>C NMR analysis was carried out as described in refs 16–22. The intrinsic viscosity  $[\eta]$  was measured in tetrahydronaphthalene at 135 °C using a standard Ubbelohde viscosimeter. The average molecular masses of i-PP samples were obtained from their intrinsic viscosity values according to  $[\eta] = K(M_v)^\alpha$ , with  $K = 1.93 \times 10^{-4}$  and  $\alpha = 0.74$ .<sup>24</sup> The SEC curves of samples show very narrow molecular mass distributions, typical of single-center zirconocene catalysts, with polydispersity indices  $M_w/M_n$  variable in the range 2–3.

The calorimetric measurements were performed with a differential scanning calorimeter (DSC) Mettler DSC-30 and Perkin-Elmer DSC-7 in a flowing N<sub>2</sub> atmosphere. The melting temperatures of the samples were taken as the peak temperature of the DSC curves recorded at 10 °C/min.

The kinetics of crystallization from the melt of the i-PP samples were studied performing melt-crystallizations at different temperatures in a differential scanning calorimeter (Mettler DSC-30). Powder samples were melted at 200 °C and kept for 5 min at this temperature in a N<sub>2</sub> atmosphere; they were then rapidly cooled to the crystallization temperature,  $T_c$ , and kept at this temperature, still in a N<sub>2</sub> atmosphere, for a crystallization time  $t$ . The samples were then heated from  $T_c$  to 200 °C at heating rate of 10 °C/min, while recording the melting enthalpy  $\Delta H(t)$  of the material crystallized at the temperature  $T_c$  during the time  $t$ . The fraction of transformed material at a given crystallization time, here and in the following defined as the “apparent crystallinity”, was calculated as a function of the crystallization time as

$$x_c'(t) = \Delta H(t)/\Delta H_m(\infty)$$

with  $1 \geq x_c'(t) \geq 0$  and  $\Delta H_m(\infty)$  the melting enthalpy of the sample fully crystallized at  $T_c$  after a very long time.

At the end of the isothermal crystallization the relative content of the  $\gamma$  form with respect to the  $\alpha$  form and the achieved total degree of crystallinity have been estimated from

the DSC curves at the latest stages of crystallization kinetics as  $f_{\gamma}(\text{DSC}) = ((\Delta H_m(\infty)_{\gamma}/(\Delta H_m^{\circ})_{\gamma})[(\Delta H_m(\infty)_{\alpha}/(\Delta H_m^{\circ})_{\alpha}) + (\Delta H_m(\infty)_{\gamma}/(\Delta H_m^{\circ})_{\gamma})]^{-1}$  and  $x_c = (\Delta H_m(\infty)/\Delta H_m^{\circ})_{\alpha} + (\Delta H_m(\infty)/\Delta H_m^{\circ})_{\gamma}$ , respectively.  $\Delta H_m(\infty)_{\alpha}$  and  $\Delta H_m(\infty)_{\gamma}$  are the melting enthalpies of crystals of  $\alpha$  and  $\gamma$  forms that develops upon completion of crystallization and have been measured from the area of the peaks present in the DSC melting curves of melt-crystallized samples performing a deconvolution of the global melting endotherm.  $(\Delta H_m^{\circ})_{\alpha}$  and  $(\Delta H_m^{\circ})_{\gamma}$  are the equilibrium melting enthalpies of  $\alpha$  and  $\gamma$  forms. The values of  $\Delta H_m^{\circ}$  of the  $\alpha$  form has been assumed equal to 209.5 J/g,<sup>25,26</sup> whereas for the  $\Delta H_m^{\circ}$  of the  $\gamma$  form the two limit values of 144.8 and 196 J/g suggested in the literature<sup>27</sup> have been considered.

The melting temperatures of the samples fully crystallized at each  $T_c$ , obtained from the maxima of endothermic peaks in the DSC heating curves measured at heating rate of 10 °C/min immediately after the completion of isothermal crystallizations, have been used in the Hoffman–Weeks method<sup>28</sup> to find the extrapolated equilibrium melting temperatures of i-PP samples of different stereoregularity.

## Results and Discussion

All the analyzed i-PP samples (Table 1) are highly regioregular and contain only mistakes in the stereoregularity consisting in isolated *rr* triad defects, whose amount depends on the structure of the catalyst (Chart 1) and conditions of polymerization.<sup>18–22</sup> The amount of *rr* defects can be varied in the range between 0.5 and 3.70 mol %, and correspondingly, the samples show melting temperatures variable between 160 and 130 °C (Table 1).

The simple microstructure of the samples allows studying the effect of the presence of *rr* defects on the kinetic of crystallization from the melt of i-PP. Moreover, the used catalysts have allowed the synthesis of samples with similar concentration of *rr* defects but different molecular weights. The effect of the molecular weight on the crystallization kinetics of i-PP has also been analyzed.

As shown in ref 16, stereodeficient i-PP samples as those of Table 1 crystallize from the melt as mixtures of  $\alpha$  and  $\gamma$  forms; the amount of  $\gamma$  form increases with increasing crystallization temperature. This indicates that the  $\gamma$  form develops preferably when the crystallization is very slow at high temperatures. Moreover, the amount of  $\gamma$  form also increases with increasing concentration of *rr* defects. In particular, the most stereoirregular sample iPP7 with *rr* content of 3.70% crystallizes from the melt almost completely in the  $\gamma$  form at crystallization temperatures higher than 100–110 °C.<sup>16</sup>

The melting behavior of metallocene made i-PPs is rather complex. Thermal analysis has indicated that i-PP samples isothermally crystallized from the melt show broad endotherms, which, depending on the degree of stereoregularity and the crystallization temperature, may be characterized by the presence of low-temperature humps and/or double melting peaks.<sup>4,11,26</sup> As an example, the DSC heating curves of melt-crystallized specimens of the most and least stereoregular samples of Table 1 (samples iPP1 with [*rr*] = 0.49% and iPP7 with [*rr*] = 3.70%) are reported in Figure 1. They have been recorded immediately after the completion of isothermal crystallizations at the indicated temperatures  $T_c$ , by heating from  $T_c$  without cooling to room temperature.

The DSC scans of the less isotactic sample iPP7, crystallized from the melt at  $T_c$  = 110 and 115 °C

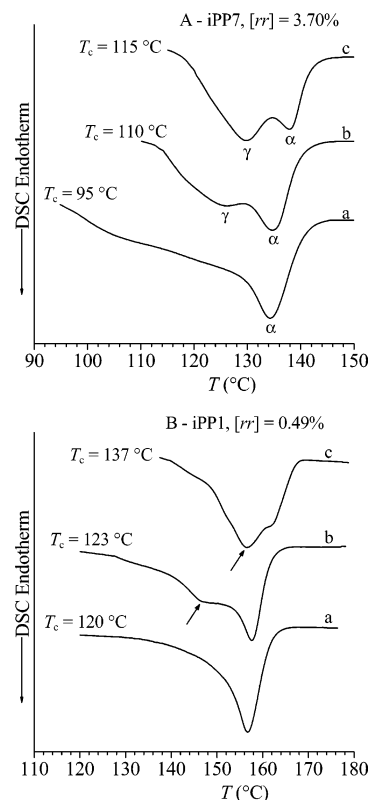


**Figure 1.** DSC heating curves recorded at heating rate of 10 °C/min immediately after completion of isothermal crystallization from the melt at the indicated crystallization temperatures  $T_c$  of specimens of the samples iPP7 (A) and iPP1 (B), with concentration of *rr* defects of 3.70 and 0.49%, respectively. In (A) the peaks at low and high temperatures (curves b and c) are attributed to the melting of crystals of  $\gamma$  and  $\alpha$  forms, respectively. In (B) the peaks indicated with arrows indicate that the samples include crystallites with different stability.

(Figure 1A, curves b and c), present endotherms with double peaks, which have been attributed in the literature to the melting of crystals of  $\gamma$  and  $\alpha$  forms,<sup>4,11</sup> according to the X-ray diffraction patterns that indicate the presence in the melt-crystallized samples of crystals of  $\alpha$  and  $\gamma$  forms.<sup>16</sup> It has been demonstrated in the literature that, at least for stereoirregular samples, only negligible recrystallization occurs during heating and the double peaks shape of the melting endotherms is basically due to the melting of different crystals.<sup>4,11</sup> The peak at low temperature is generally attributed to the melting of the  $\gamma$  form, whose crystals always contain  $\alpha/\gamma$  structural disorder,<sup>11</sup> whereas the high-temperature peak is attributed to the melting of the more ordered crystals of  $\alpha$  form.<sup>4,11</sup> This interpretation has been basically confirmed by the fact that the contents of the  $\gamma$  form evaluated, as explained in the Experimental Section, from the DSC curves b and c of Figure 1A ( $f_{\gamma}(\text{DSC})$  = 75 and 88%, respectively, assuming  $(\Delta H_m^{\circ})_{\gamma}$  = 196 J/g, or  $f_{\gamma}(\text{DSC})$  = 70 and 84%, respectively, assuming  $(\Delta H_m^{\circ})_{\gamma}$  = 144.8 J/g), are in good agreement with the values of 75 and 86%, respectively, evaluated in ref 16 from the X-ray diffraction profiles. The melting of crystallites of  $\gamma$  form formed at  $T_c$  = 95 °C is less evident (curve a of Figure 1A) because the relative amount of  $\gamma$  form which develops at this temperature for the sample iPP7 is below 20%.<sup>16</sup>

The DSC scans of specimens of the most isotactic sample iPP1 crystallized at low temperatures present a single melting peak (curve a of Figure 1B). At

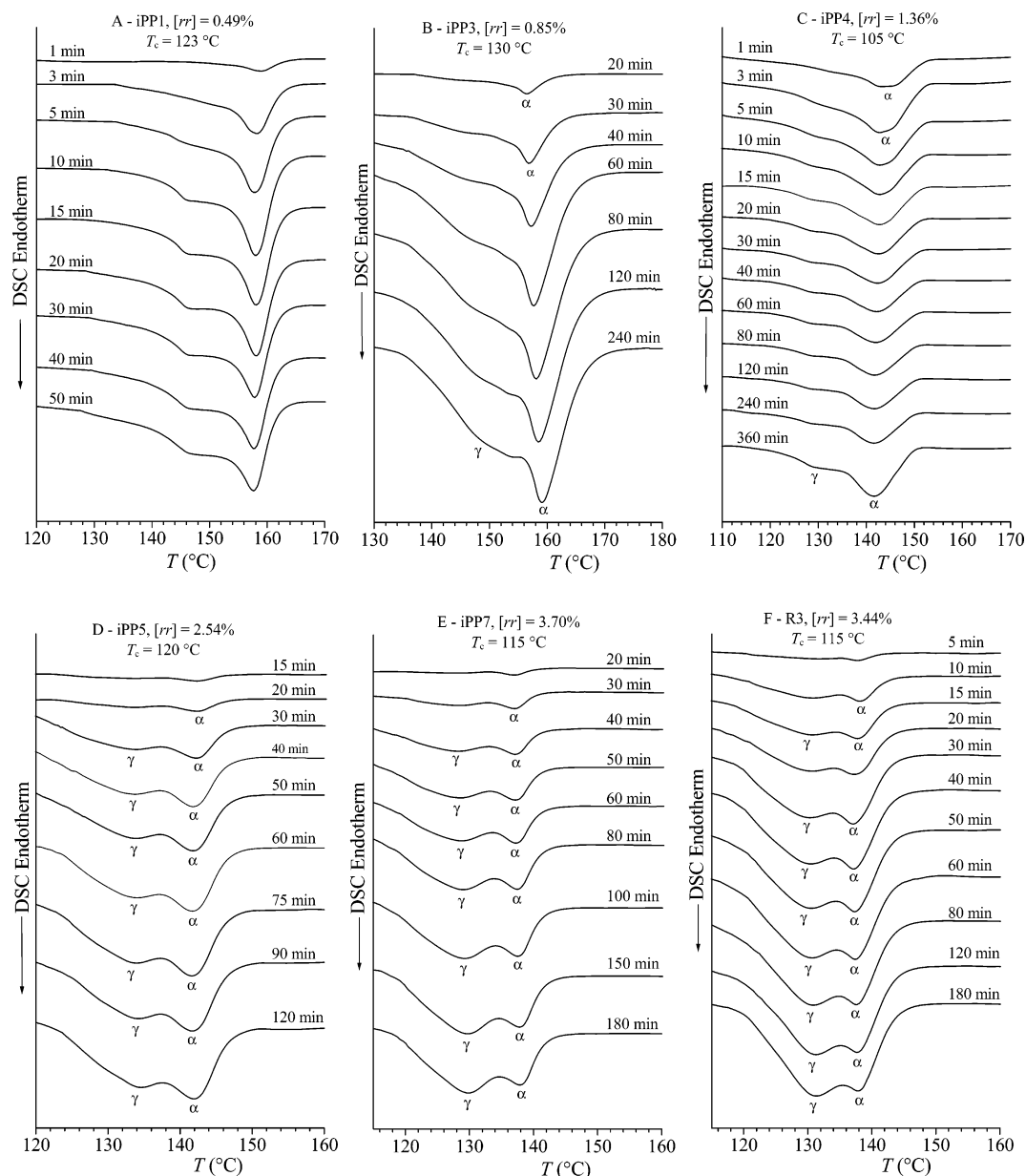


**Figure 2.** DSC heating scans of i-PP samples isothermally crystallized from the melt at different crystallization temperatures  $T_c$  during the indicated crystallization time: (A) sample iPP1 with  $[rr] = 0.49\%$ ; (B) sample iPP3 with  $[rr] = 0.85\%$ ; (C) sample iPP4 with  $[rr] = 1.36\%$ ; (D) sample iPP5 with  $[rr] = 2.54\%$ ; (E) sample iPP7 with  $[rr] = 3.70\%$ ; (F) sample R3 with  $[rr] = 3.44\%$ .

crystallization temperatures above  $125\text{ }^{\circ}\text{C}$ , besides the melting peak at high temperature, a second broad endotherm is present at low temperatures (curve b of Figure 1B). The area of the low-temperature peak increases, and that of the high-temperature peak decreases, with increasing the crystallization temperature (curve c of Figure 1B). Since the sample iPP1 crystallizes mainly in the  $\alpha$  form and the amount of  $\gamma$  form is very low (less than 20%) at any crystallization temperature,<sup>16</sup> the low-temperature endotherm cannot be attributed to the melting of crystals of  $\gamma$  form. Moreover, detailed analyses by Strobl et al.<sup>29</sup> have indicated that for highly stereoregular iPP samples crystallized at high crystallization temperatures, when mainly the  $\alpha$  form is obtained, no relevant recrystallization occurs during melting, and the observed complex melting endotherms is rather due to the presence of crystallites of different stability formed during the crystallization.<sup>29</sup> More precisely, Strobl et al. suggested that three types of crystallites generally form: (i) the dominant crystallites

growing in radial direction along the radius of the spherulites at the begin of crystallization, (ii) “subsidiary” crystallites, also oriented in radial direction, formed subsequently by insertion, and (iii) less stable tangential crystallites oriented with their surfaces in the transverse direction, forming the characteristic crosshatch morphology. According to small-angle X-ray diffraction<sup>29</sup> and optical microscope<sup>30</sup> experiments, the broad peak at low temperatures in the DSC curves is due to the melting of the less stable tangential lamellae and of “subsidiary” radial lamellae, whereas the radial dominant lamellae formed at the begin of crystallization melt at higher temperatures.

Probably the origin of the complex melting behavior of the sample iPP1 in the DSC curves b and c of Figure 1B is due to the presence of crystallites of different stability melting at different temperatures. The less stable crystals melting at low temperatures are in part of the  $\alpha$  form, in part of the  $\gamma$  form, whereas the most stable crystals melting at high temperatures are of the



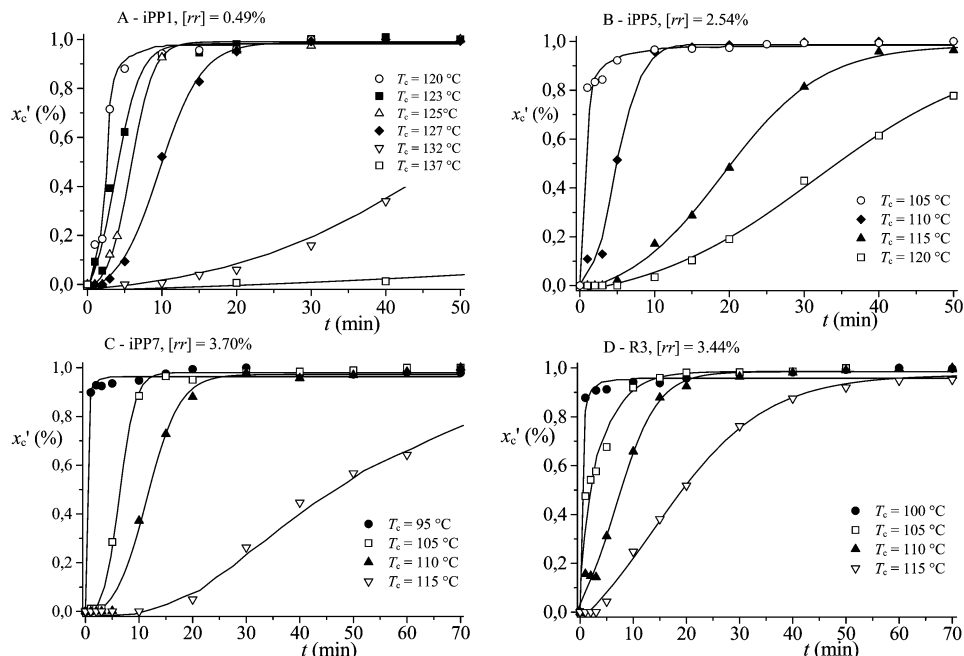


**Figure 3.** Apparent crystallinity  $x_c'(t)$  as a function of the crystallization time for i-PP samples isothermally crystallized from the melt at different crystallization temperatures  $T_c$ : (A) sample iPP1 with  $[rr] = 0.49\%$ ; (B) sample iPP5 with  $[rr] = 2.54\%$ ; (C) sample iPP7 with  $[rr] = 3.70\%$  and  $M_v = 202\,400$ ; (D) sample R3 with  $[rr] = 3.44\%$  and  $M_v = 66\,000$ .

$\alpha$  form and form originally at the crystallization temperature  $T_c$ .

Samples of highly stereoregular i-PP crystallized at low temperatures (for instance, curve a of Figure 1B) are instead characterized by less stable crystallites that undergo repeated melting–recrystallization processes during heating at relatively low heating rate.<sup>29</sup> The original crystallites grown at  $T_c$  partially melt and recrystallize with formation of new thicker lamellae that melt at higher temperatures.<sup>29</sup> As observed by Strobl,<sup>29</sup> at high heating rates, for instance at  $10\text{ }^\circ\text{C/min}$ , recrystallization may be almost completely suppressed, so that one has again a simple melting. At heating rate of  $10\text{ }^\circ\text{C/min}$  we have observed that superheating may be less than  $4\text{ }^\circ\text{C}$ .

The melting behavior of the less stereoregular samples iPP4–iPP6 and R3, with  $rr$  content in the range between 1 and  $3.70\%$ , is similar to that of the sample iPP7 (Figure 1A). These samples crystallize at any crystallization temperature as mixtures of  $\alpha$  and  $\gamma$  forms<sup>11,16</sup> and show DSC heating curves characterized by the presence of double peaks due to the melting of the  $\alpha$  and  $\gamma$  forms, and only negligible recrystallization occurs during heating. The melting behavior of the more stereoregular samples iPP2 and iPP3, with  $rr$  contents less than  $1\%$ , is instead similar to that of the sample iPP1 (Figure 1B). These samples crystallize mainly in the  $\alpha$  form at any crystallization temperature;<sup>16</sup> crystals of different stability and melting temperatures form at high crystallization temperatures, and no significant recrystallization occurs during heating. At low crystallization temperatures, instead, less stable crystals are obtained, and recrystallization may occur during heating at low heating rate.

Understanding the melting behavior of i-PP of different stereoregularity allows interpreting the effect of stereodefects on the crystallization kinetics. Examples of crystallization kinetics for some samples of Table 1 are reported in Figures 2 and 3. The samples have been isothermally crystallized in DSC at the crystallization

temperature  $T_c$  for a time  $t$  and then heated from  $T_c$  up to  $200\text{ }^\circ\text{C}$  at heating rate of  $10\text{ }^\circ\text{C/min}$ , while recording the melting enthalpy. The amount of materials crystallized at  $T_c$  during the time  $t$  has been evaluated from the measure of the melting enthalpy.

The DSC heating scans, from  $T_c$  after the crystallization time  $t$ , are shown in Figure 2. In all cases the positions of the melting peaks do not change with crystallization time. As discussed above and shown in Figure 1A, the total melting process of more stereoregular samples is characterized by endotherms with double peaks corresponding to the melting of crystals of  $\alpha$  and  $\gamma$  forms produced during the isothermal melt-crystallization (Figure 2C–F). At any crystallization time we can assume that the peak at low temperature corresponds to the melting of disordered crystals of  $\gamma$  form, whereas that at high temperature corresponds to the melting of  $\alpha$  form.<sup>4,11</sup> For more isotactic samples that crystallize basically in the  $\alpha$  form,<sup>16</sup> the multiple peaks observed in the DSC scans of Figure 2A,B are largely due to crystals of  $\alpha$  form of different stability. The most stable crystals melting at higher temperature are dominant radial lamellae of  $\alpha$  form that form originally at  $T_c$ , as indicated by the fact the high-temperature peak is present in the DSC curves since the early stages of crystallization (Figure 2A,B).

The maximum degree of crystallinity achieved during isothermal crystallizations, estimated from the melting enthalpies of crystals of  $\alpha$  and  $\gamma$  forms which develops upon completion of isothermal crystallization, measured in the DSC scans at the latest stages of crystallization kinetics of Figure 2, increases with increasing stereoregularity, from  $35\text{--}45\%$  (samples iPP5–iPP7) to  $40\text{--}50\%$  (samples iPP1–iPP3), also in agreement with results of X-ray diffraction analysis of ref 16.

Since in the present study we are interested in the analysis of the kinetics of crystallization of i-PP as a function of concentration of  $rr$  defects variable in a wide range ( $0.49\text{--}3.70\text{ mol } \%$ ), we have studied the global crystallization kinetics, independent of the number and

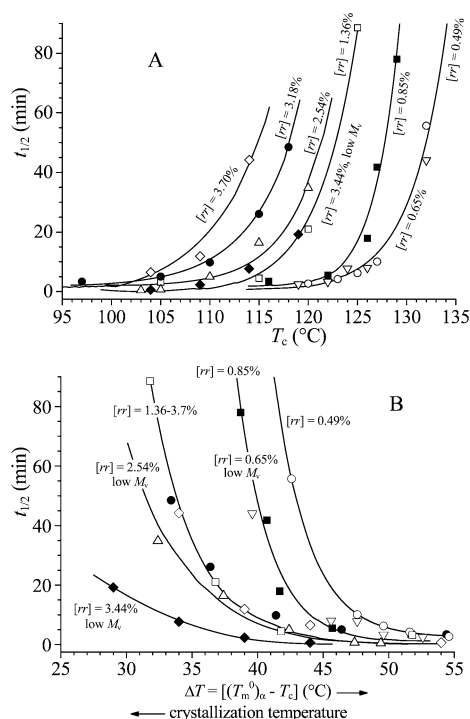


**Figure 4.** Half-crystallization time  $t_{1/2}$  as a function the crystallization temperature  $T_c$  (A) and of the undercooling  $\Delta T = [(T_m^0)_{\alpha} - T_c]$  (B), for i-PP samples isothermally crystallized from the melt: (○) sample iPP1 with  $[rr] = 0.49\%$ , (▽) sample iPP2 with  $[rr] = 0.65\%$  and  $M_v = 108\,900$ ; (■) sample iPP3 with  $[rr] = 0.85\%$ ; (□) sample iPP4 with  $[rr] = 1.36\%$ ; (△) sample iPP5 with  $[rr] = 2.54\%$  and  $M_v = 106\,000$ ; (●) sample iPP6 with  $[rr] = 3.18\%$  and  $M_v = 222\,800$ ; (◇) sample iPP7 with  $[rr] = 3.70\%$  and  $M_v = 202\,400$ ; (◆) sample R3 with  $[rr] = 3.44\%$  and  $M_v = 66\,000$ .

amount of crystalline phases which develop during isothermal crystallization. We did not monitor the development of the  $\alpha$  and  $\gamma$  forms as a function of time, as made for instance by Alamo et al.,<sup>4</sup> because this analysis can be accurately performed (using the DSC techniques) only for samples showing well-separated melting peaks of the two forms. Such kind of analysis, indeed, would be restricted only to samples with contents of stereodefects variable in a narrow range ( $rr$  concentration between 2 and 4 mol %)<sup>4,16</sup> and to a narrow range of crystallization temperature, preventing a direct comparison of the crystallization kinetics of i-PP samples of very different stereoregularity. For these reasons we have only evaluated the increase of the total apparent crystallinity  $x_c'(t)$  during time from the global melting enthalpies of the two crystalline forms in the DSC scans of the kind of Figure 2. The apparent crystallinity  $x_c'(t)$  is reported, for some samples of Table 1, in Figure 3 as a function of the crystallization time for various crystallization temperatures.

The values of the half-crystallization time  $t_{1/2}$  (time at which half of the crystallizable materials is crystallized) are reported in Figure 4A as a function of the crystallization temperature. It is apparent from Figure 4A that at low values of crystallization temperature, in conditions of fast crystallization, similar crystallization rates are observed for all samples regardless of the microstructure (molecular mass and concentration of  $rr$  defects). At high crystallization temperatures the crystallization rate seems to decrease with increasing concentration of  $rr$  defects. At the same values of the crystallization temperature  $T_c$  the crystallization time,

indeed, increases with increasing concentration of  $rr$  defects.

As a matter of fact, the curves of Figure 4A show a constant shape and are only shifted toward lower values of the crystallization temperature with increasing concentration of  $rr$  defects. The horizontal shift is quite expected because the melting temperature of the samples decreases with decreasing stereoregularity (Table 1) and lower values of crystallization temperature are accessible. Therefore, the horizontal shift of the curves of Figure 4A could be only related to the different values of undercooling ( $T_m^0 - T_c$ ) if we assume that samples of i-PP of different stereoregularity have different values of the equilibrium melting temperature  $T_m^0$ , as found by Cheng<sup>26c</sup> and also reported in the case of syndiotactic polypropylene.<sup>31</sup> However, lack of vertical shift and invariance of shape of curves of Figure 4A are quite surprising, since our samples develop different amounts of  $\alpha$  and  $\gamma$  forms at different crystallization temperatures and, at a given crystallization temperature, for different stereoregularity. This behavior is similar to that observed by Strobl in the case of syndiotactic copolymers of propylene with 1-octene.<sup>32</sup>

The shape of the curves of Figure 4A suggests the existence, for each sample, of a limit temperature with zero crystallization rate corresponding to infinite  $t_{1/2}$ . For systems that crystallize in a single phase, this limit temperature should correspond to the equilibrium melting temperature.<sup>33</sup> In our case two different crystalline  $\alpha$  and  $\gamma$  forms are generally obtained. According to Mezghani and Phillips,<sup>27</sup> the equilibrium melting temperatures of  $\alpha$  and  $\gamma$  forms of fully isotactic polypropylene are 186.1 and 187.2 °C, respectively, also in agreement with other similar values for the  $\alpha$  form of nearly 185 °C reported by Cheng et al.<sup>26b,c</sup> and of 186 °C reported many years before.<sup>34</sup>

The determination of the limit temperature by extrapolation of curves of Figure 4A to zero crystallization rate, following for instance the procedure suggested by Strobl,<sup>32,33</sup> would lead to too large errors. Furthermore, on inspection of Figure 4A, we notice that the horizontal displacements of the kinetic curves vary with the content of stereodefects, ranging from  $\approx 4$  °C (between curves of samples iPP1–iPP2, with  $[rr] \approx 0.5\%$  and sample iPP3 with  $[rr] \approx 1\%$ ) to  $\approx 18$  °C (between curves of sample iPP1 and sample iPP7 with  $[rr] \approx 4\%$ ). A comparison with the corresponding changes of the melting temperatures ( $T_m$ ) of the as-prepared samples (Table 1) shows that the shift of crystallization rate curves is much lower than the differences in the melting temperature values. This probably indicates that the difference of the crystallization rate of samples having different stereoregularity (Figure 4A) cannot be ascribed only to the different values of undercooling.

The values of undercooling ( $T_m^0 - T_c$ ) can be determined only if the equilibrium melting temperatures of  $\alpha$  and  $\gamma$  forms for i-PP samples of different stereoregularity are known. The values of the  $T_m^0$  may be determined upon application of the Hoffman–Weeks standard method<sup>28</sup> using the melting temperatures of samples crystallized from the melt at different  $T_c$ , which can be obtained from the maxima of the endothermic peaks in the DSC heating curves recorded from  $T_c$  immediately after the completion of isothermal crystallizations without cooling to room temperature (as in Figure 1). In this analysis we have taken into account only the peak in the DSC curves that can be attributed to the melting of

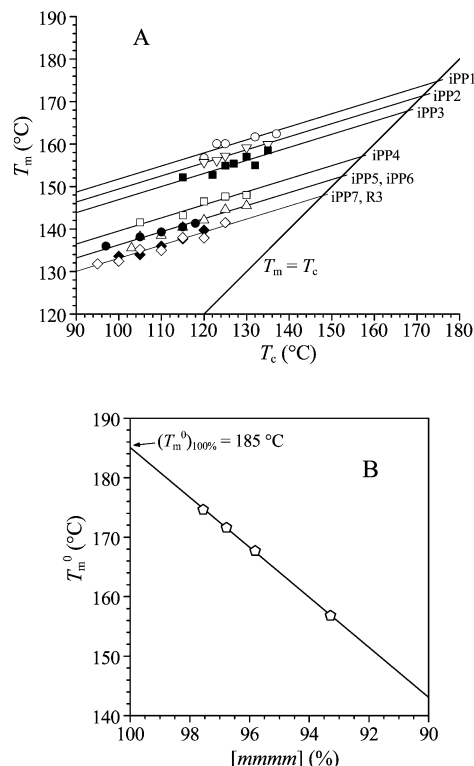


**Figure 5.** (A) Melting temperature  $T_m$  of specimens of i-PP samples of different stereoregularity isothermally crystallized from the melt, measured from the DSC curves recorded at heating rate of 10 °C/min immediately after completion of crystallization, as a function of the crystallization temperature  $T_c$ . Extrapolation to the line  $T_m = T_c$  are also drawn. (○) Sample iPP1 with  $[rr] = 0.49\%$ , (▽) sample iPP2 with  $[rr] = 0.65\%$ ; (■) sample iPP3 with  $[rr] = 0.85\%$ ; (□) sample iPP4 with  $[rr] = 1.36\%$ ; (△) sample iPP5 with  $[rr] = 2.54\%$ ; (●) sample iPP6 with  $[rr] = 3.18\%$ ; (◇) sample iPP7 with  $[rr] = 3.70\%$ ; (◆) sample R3 with  $[rr] = 3.44\%$ . (B) Extrapolated equilibrium melting temperatures  $T_m^0$  (○) of the samples iPP1, iPP2, iPP3, and iPP4 (from part A) as a function of the concentration of the fully isotactic pentads  $mmmm$ . Extrapolation to  $[mmmm] = 100\%$  gives the equilibrium melting temperature of  $\alpha$  form for the fully isotactic polypropylene  $(T_m^0)_{100\%}$ .

the original crystallites grown at each  $T_c$ . As discussed above (Figure 1), this attribution is straightforward for the low stereoregular samples at any crystallization temperature and for more stereoregular samples crystallized at high  $T_c$ , where no significant recrystallization occurs during heating. For the more stereoregular samples crystallized at low  $T_c$  a reliable attribution may be done, provided that the DSC curves are measured at the heating rate of 10 °C/min in order to prevent the occurrence of recrystallization. We have checked that at this heating rate superheating effects are not higher than 4 °C for all samples.

The melting temperatures of crystals of the  $\alpha$  form  $(T_m)_\alpha$  of the melt-crystallized i-PP samples of Table 1 are reported in Figure 5A as a function of the crystallization temperature  $T_c$ . The data are well-fitted by nearly parallel straight lines, as reported by Cheng et al. for different i-PP samples of different isotacticity.<sup>26c</sup> The extrapolation to the line  $T_m = T_c$  gives the values of equilibrium melting temperatures  $(T_m^0)_\alpha$  of  $\alpha$  form for i-PP samples having different concentrations of  $rr$  stereodefects. The so-obtained  $(T_m^0)_\alpha$  values are reported in Table 1, whereas those of the more stereoregular samples are plotted in Figure 5B as a function of

the degree of stereoregularity, expressed as concentration of the fully isotactic pentad  $mmmm$ . The extrapolation of these data to  $[mmmm] = 100\%$  provides the value of  $(T_m^0)_{100\%} = 185$  °C for the equilibrium melting temperature of the fully isotactic polypropylene (Figure 5B), in good agreement with the values reported in the literature.<sup>26,27,34</sup> This indicates that reasonable values of the equilibrium melting temperature  $(T_m^0)_\alpha$  have been obtained from Figure 5A.

The Hoffman–Weeks extrapolation method could not be applied to obtain the equilibrium melting temperature of the  $\gamma$  form of i-PP samples of different stereoregularity, because the data of the melting temperature of the peaks attributed to the  $\gamma$  form (clearly visible in the DSC curves of melt-crystallized specimens of low stereoregular samples iPP4–iPP7) as a function of crystallization temperature  $T_c$  are fitted by lines nearly parallel to the line  $T_m = T_c$ . This is probably due to the fact that the  $\gamma$  form crystallized in low stereoregular i-PP samples contains large amounts of structural disorder that, in addition, change with the crystallization temperature, preventing a reliable extrapolation. However, the values of  $(T_m^0)_\gamma$  of the  $\gamma$  form for i-PP samples having different concentrations of  $rr$  defects are expected to be not very different from the values of  $(T_m^0)_\alpha$  of the  $\alpha$  form because of the similar structural features of the two forms, the similar packing energy,<sup>35</sup> and the similar values of the equilibrium melting temperatures of  $\alpha$  and  $\gamma$  forms (186.1 and 187.2 °C, respectively) for the fully isotactic polypropylene reported by Mezghani and Phillips.<sup>27</sup>

Once the values of the equilibrium melting temperatures have been determined, quantitative values of the undercooling can be calculated and the crystallization rate of samples of different stereoregularity of Figure 4A can be compared at the same undercooling. The values of the half-crystallization time  $t_{1/2}$  are reported in Figure 4B as a function of the undercooling  $\Delta T = [(T_m^0)_\alpha - T_c]$ . It is apparent that the data are not fitted by a single curve, but at similar values of  $\Delta T = [(T_m^0)_\alpha - T_c]$  the crystallization time decreases with increasing concentration of  $rr$  defects. Therefore, even though the overall degree of crystallinity decreases, the crystallization rate increases with increasing concentration of  $rr$  defects, at least at high values of crystallization temperatures. Moreover, the data of Figure 4B also indicate that for samples having similar concentration of  $rr$  defects the crystallization rate is higher for samples with lower molecular mass (compare for instance in Figure 4B the samples iPP1 and iPP2 having  $[rr] = 0.49$  and 0.65%, respectively, and molecular masses  $M_v = 195\,700$  and 108 900, respectively, or the samples iPP6 and iPP5 with  $[rr] = 3.18$  and 2.54%, respectively, and molecular masses  $M_v = 222\,800$  and 106 000, respectively, or the samples iPP7 and R3 having  $[rr] = 3.70\%$  and 3.44%, respectively, and molecular masses  $M_v = 202\,400$  and 66 000, respectively).

The unexpected experimental result that the presence of  $rr$  defects induces increase of crystallization rate could be probably explained considering that these stereodefects are highly tolerated in the crystalline lattices of  $\alpha$  and  $\gamma$  forms of i-PP and produces increase of chain flexibility due to the increase in the defective i-PP chains of the number of bonds in the *trans*-planar conformation. In fact, as suggested by us in ref 9, the backbone torsion angles of bonds close to the  $rr$  triad defects are very likely in the *trans*-planar conformation.



As expected, the effect of the presence of *rr* defects and molecular weight is remarkable at high crystallization temperatures, when the crystallization is slow, but it is negligible at low crystallization temperatures in condition of fast crystallization.

An analysis of the data of Figure 2 also reveals that for all the samples crystallized from the melt the melting endotherms of the materials crystallized in the first minutes of the crystallization present only the peak at high temperature, corresponding to the melting of crystals of  $\alpha$  form. The peak at low temperatures, which corresponds to the melting of the  $\gamma$  form for the samples of low stereoregularity, appears in the DSC curves of Figure 2C–F only for longer crystallization times. This indicates that during the isothermal crystallization from the melt crystals of  $\alpha$  form develop at the beginning of the crystallization, whereas the formation of crystals of  $\gamma$  form is observed only at longer crystallization times. It is worth noting that, even in the case of irregular samples, for instance the sample iPP7 containing 3.70% of *rr* defects, which, as discussed before, crystallizes at high temperatures in mixture of  $\alpha$  and  $\gamma$  forms with higher amount of  $\gamma$  form, a small amount of crystals of  $\alpha$  form develops at beginning of the crystallization (Figure 2E). With increasing crystallization time the area of the low-temperature peak of the  $\gamma$  form in the DSC curves of Figure 2E increases and becomes larger than that of the  $\alpha$  form.

These data indicate that the crystals of  $\gamma$  form are probably nucleated over the preformed crystals of  $\alpha$  form. At the end of the crystallization the relative area of the two peaks correspond to a fraction of  $\gamma$  form similar to that calculated from the X-ray diffraction patterns.<sup>16</sup> Our observation that the  $\gamma$  form nucleated on preformed crystals of  $\alpha$  form is consistent with results reported by Lotz et al.,<sup>36</sup> and more recently confirmed by Thomann et al.,<sup>3</sup> that crystals of  $\alpha$  form are formed first and those of the  $\gamma$  form crystallize in a second stage on the lateral (010) growth faces of  $\alpha$  crystals. The nucleation of  $\gamma$  form over the preformed crystals of  $\alpha$  form also suggests a common crystallization mechanism for the two polymorphs, involving cross-hatching,<sup>37</sup> which accounts for the invariance of shape of kinetic curves of Figure 4A. The occurrence of transverse crystallites during crystallization of the  $\alpha$  form, as arising from the epitaxial crystallization mechanism of daughter lamellae on mother lamellae of  $\alpha$  form,<sup>37</sup> producing nearly perpendicular orientation of chain axes, is totally consistent with the growth of crystals of  $\gamma$  form, having perpendicular orientation of chains at molecular level, on preformed lamellae of  $\alpha$  form.<sup>36</sup>

It is worth noting that the observation by Alamo et al.<sup>4</sup> that the initial crystallization rates of  $\alpha$  and  $\gamma$  forms are virtually identical is probably relative to a stage of the crystallization kinetic which follows the nucleation of  $\gamma$  form crystals over the preformed  $\alpha$  form crystals.

## Conclusions

Polypropylene samples with controlled microstructure have been obtained with a series of regiospecific metallocene catalysts. The samples are highly regioregular and contain only *rr* defects of stereoregularity in a wide range of concentration, with melting temperatures ranging between 160 and 130 °C. The produced samples and the simple microstructure have allowed studying the relationships between kinetics of melt-crystalliza-

tion and the microstructure of polypropylene chains. The effects of the presence of *rr* defects and of the molecular mass on the kinetic of crystallization from the melt have been studied.

The samples have been isothermally crystallized from the melt and the values of the equilibrium melting temperatures for i-PP of different stereoregularity have been estimated with the Hoffman–Weeks method. The kinetic study has shown that the crystallization rate increases with increasing the concentration of *rr* defects and decreasing the molecular mass. The effect of the *rr* defects is probably related to the increase of chain flexibility due to the high concentration of bonds in *trans*-planar conformation close to the *rr* triad defects.

The kinetic data also indicate that, for the i-PP samples that crystallize from the melt as a mixture of  $\alpha$  and  $\gamma$  forms, crystals of  $\alpha$  form develop at the beginning of the crystallization, whereas the formation of crystals of  $\gamma$  form is observed only at longer crystallization times. According to the literature, the crystals of  $\gamma$  form are nucleated over the preformed crystals of  $\alpha$  form.

**Acknowledgment.** Financial support from Basell Polyolefins (Ferrara, Italy) and from the “Ministero dell’Istruzione, dell’Università e della Ricerca” of Italy (PRIN 2004 project) is gratefully acknowledged. We thank Isabella Camurati for the <sup>13</sup>C NMR analysis of the i-PP samples and Ilya Nifant’ev, Simona Guidotti, and Francesca Focante for the synthesis of the zirconocenes.

## References and Notes

- Resconi, L.; Cavallo, L.; Fait, A.; Piemontesi, F. *Chem. Rev.* **2000**, *100*, 1253.
- Fischer, D.; Mülhaupt, R. *Macromol. Chem. Phys.* **1994**, *195*, 1433.
- Thomann, R.; Wang, C.; Kressler, J.; Mülhaupt, R. *Macromolecules* **1996**, *29*, 8425.
- Alamo, R. G.; Kim, M. H.; Galante, M. J.; Isasi, J. R.; Mandelkern, L. *Macromolecules* **1999**, *32*, 4050.
- VanderHart, D. L.; Alamo, R. G.; Nyden, M. R.; Kim, M. H.; Mandelkern, L. *Macromolecules* **2000**, *33*, 6078.
- Alamo, R. G.; VanderHart, D. L.; Nyden, M. R.; Mandelkern, L. *Macromolecules* **2000**, *33*, 6094.
- Thomann, R.; Semke, H.; Maier, R. D.; Thomann, Y.; Scherble, J.; Mülhaupt, R.; Kressler, J. *Polymer* **2001**, *42*, 4597.
- Hosier, I. L.; Alamo, R. G.; Estes, P.; Isasi, G. R.; Mandelkern, L. *Macromolecules* **2003**, *36*, 5623.
- Auriemma, F.; De Rosa, C.; Boscato, T.; Corradini, P. *Macromolecules* **2001**, *34*, 4815.
- De Rosa, C.; Auriemma, F.; Circelli, T.; Waymouth, R. M. *Macromolecules* **2002**, *35*, 3622.
- Auriemma, F.; De Rosa, C. *Macromolecules* **2002**, *35*, 9057.
- De Rosa, C.; Auriemma, F.; Circelli, T.; Longo, P.; Boccia, A. C. *Macromolecules* **2003**, *36*, 3465.
- De Rosa, C.; Auriemma, F.; Spera, C.; Talarico, G.; Tarallo, O. *Macromolecules* **2004**, *37*, 1441.
- De Rosa, C.; Auriemma, F.; Spera, C.; Talarico, G.; Gahleitner, M. *Polymer* **2004**, *45*, 5875.
- De Rosa, C.; Auriemma, F.; Perretta, C. *Macromolecules* **2004**, *37*, 6843.
- De Rosa, C.; Auriemma, F.; Di Capua, A.; Resconi, L.; Guidotti, S.; Camurati, I.; Nifant’ev, I. E.; Laishevtsev, I. P. *J. Am. Chem. Soc.* **2004**, *126*, 17040.
- De Rosa, C.; Auriemma, F.; De Lucia, G.; Resconi, L. *Polymer* **2005**, *46*, 9461.
- Resconi, L.; Piemontesi, F.; Camurati, I.; Sudmeijer, O.; Nifant’ev, I. E.; Ivchenko, P. V.; Kuz'mina, L. G. *J. Am. Chem. Soc.* **1998**, *120*, 2308.
- Resconi, L.; Balboni, D.; Baruzzi, G.; Fiori, C.; Guidotti, S. *Organometallics* **2000**, *19*, 420.
- Nifant’ev, I. E.; Guidotti, S.; Resconi, L.; Laishevtsev, I. (Basell: Italy) PCT Int. Appl. WO 01/47939, 2001. Fritze, C.;



- Resconi, L.; Schulte, J.; Guidotti, S. (Basell: Italy) PCT Int. Appl. WO 03/00706, 2003.
- (21) Resconi, L.; Guidotti, S.; Camurati, I.; Nifant'ev, I. E.; Laishchev, I. *Polym. Mater. Sci. Eng.* **2002**, *87*, 76.
- (22) Nifant'ev, I. E.; Laishchev, I. P.; Ivchenko, P. V.; Kashulin, I. A.; Guidotti, S.; Piemontesi, F.; Camurati, I.; Resconi, L.; Klusener, P. A. A.; Rijsemus, J. J. H.; de Kloe, K. P.; Korndorffer, F. M. *Macromol. Chem. Phys.* **2004**, *205*, 2275.
- Resconi, L.; Guidotti, S.; Camurati, I.; Frabetti, R.; Focante, F.; Nifant'ev, I. E.; Laishchev, I. P. *Macromol. Chem. Phys.* **2005**, *206*, 1405.
- (23) Covezzi, M.; Fait, A. (Basell-Italy) PCT Int. Appl. WO 01/44319, 2001.
- (24) Moraglio, G.; Gianotti, G.; Bonicelli, U. *Eur. Polym. J.* **1973**, *9*, 693.
- (25) Wunderlich, B. In *Macromolecular Physics*; Academic Press: New York, Vol. I, 1973; p 63. Bu, H. S.; Cheng, S. Z. D.; Wunderlich, B. *Makromol. Chem., Rapid. Commun.* **1988**, *9*, 75.
- (26) (a) Janimak, J. J.; Cheng, S. Z. D. *Polym. Bull. (Berlin)* **1989**, *22*, 95. (b) Cheng, S. Z. D.; Janimak, J. J.; Zhang, A.; Cheng, H. N. *Macromolecules* **1990**, *23*, 298. (c) Cheng, S. Z. D.; Janimak, J. J.; Zhang, A.; Hsieh, E. T. *Polymer* **1991**, *32*, 648. (d) Janimak, J. J.; Cheng, S. Z. D.; Giusti, P. A.; Hsieh, E. T. *Macromolecules* **1991**, *24*, 2253. (e) Janimak, J. J.; Cheng, S. Z. D.; Zhang, A.; Hsieh, E. T. *Polymer* **1992**, *33*, 728.
- (27) Mezghani, K.; Phillips, P. J. *Polymer* **1998**, *39*, 3735.
- (28) Hoffman, J. D.; Weeks, J. J. *J. Res. Natl. Bur. Stand.* **1962**, *66A*, 13.
- (29) Iijima, M.; Strobl, G. *Macromolecules* **2000**, *33*, 5204.
- (30) Alamo, R. G.; Brown, G. M.; Mandelkern, L.; Lehtinen, A.; Paukkeri, R. *Polymer* **1999**, *40*, 3933. White, H. M.; Bassett, D. C. *Polymer* **1997**, *38*, 5515.
- (31) De Rosa, C.; Auriemma, F.; Vinti, V.; Galimberti, M. *Macromolecules* **1998**, *31*, 6206.
- (32) Hauser, G.; Schmidtke, J.; Strobl, G. *Macromolecules* **1998**, *31*, 6250.
- (33) Strobl, G. *The Physics of Polymers*; Springer: Berlin, 1997.
- (34) Petraccone, V.; Guerra, G.; De Rosa, C.; Tuzi, A. *Macromolecules* **1985**, *18*, 813.
- (35) Ferro, D. R.; Brückner, S.; Meille, S. V.; Ragazzi, M. *Macromolecules* **1992**, *25*, 5231.
- (36) Lotz, B.; Graff, S.; Straupé, C.; Wittmann, J. C. *Polymer* **1991**, *32*, 2902.
- (37) Lotz, B.; Wittmann, J. C. *J. Polym. Sci., Polym. Phys. Ed.* **1986**, *24*, 1541.

MA0510845